Original published in Journal of Structural Biology 160: 190-199 (2007)

Mechanism of osmoprotection by archaeal S-layers: A theoretical study

Harald Engelhardt

Max-Planck-Institut für Biochemie, D-82152 Martinsried, Germany

MPI für Biochemie, Am Klopferspitz 18, D-82152 Martinsried, Germany
Tel. +49 89 8578 2650, Fax +49 89 8578 2641, engelhar@biochem.mpg.de

Abstract

Many *Archaea* possess protein surface layers (S-layers) as the sole cell wall component. S-layers must therefore integrate the basic functions of mechanical and osmotic cell stabilisation. While the necessity is intuitively clear, the mechanism of structural osmoprotection by S-layers has not been elucidated yet. The theoretical analysis of a model S-layer-membrane assembly, derived from the typical cell envelope of *Crenarchaeota*, explains how S-layers impart lipid membranes with increased resistance to internal osmotic pressure and offers a quantitative assessment of S-layer stability. These considerations reveal the functional significance of S-layer symmetry and unit cell size and shed light on the rationale of S-layer architectures.

Keywords

prokaryotic cell envelope, prokaryotic cell wall, S-layer-membrane assembly, S-layer structure, S-layer function, S-layer stability, osmotic pressure

1. Introduction

Prokaryotes have adopted a repertoire of mechanisms that enable them to cope with the challenges of changing osmotic conditions (Göller et al., 1998; Martin et al., 1999; Müller et al., 2005). These mechanisms comprise adaptation by osmosensing and synthesis of compatible solutes (Müller et al., 2005), ion accumulation, activation of mechanosensitive membrane proteins (Blount et al., 1996), and the rigid cell wall as structural osmoprotectant. The adaptation machineries actively respond to osmotic stress and trigger the internal conditions such that they keep the osmotic pressure within the physiological range. The cell wall apparently compensates for residual pressure and for rapid turgour fluctuations.

Gram-negative bacteria exhibit a turgour of up to $6 \cdot 10^5$ Pa (Koch and Pinette, 1987; Overmann et al., 1991) and Gram-positive bacteria of $\approx 20 \cdot 10^5$ Pa (Beveridge, 1988). Some measurements even suggest pressures of $\approx 100 \cdot 10^5$ Pa or higher (Arnoldi et al., 2000; Xu et al., 1996). While the peptidoglycan network compensates for pressure differences in bacteria (Engelhardt, 2007), the situation is quite different for archaea, with S-layers as the sole cell wall component (Fig. 1). The apparent archaeal periplasmic space is more "leaky" because of the higher porosity of S-layers compared to porins in outer membranes (Engelhardt and Peters, 1998), and is probably not correspondingly equipped with charged molecules to balance the osmotic milieu with the cytoplasm. The turgour predominantly acts on the cell membrane, and archaea that are devoid of other cell wall components must therefore rely on surface proteins as structural osmoprotectants. The S-layer-membrane assembly displayed in Fig. 1A is typical for most of the *Crenarchaeota,* for some *Euryarchaeota*, and for *Nanoarchaeum equitans*, the sole representative of the recently defined *Nanoarchaeota* (Huber et al., 2002). The mechanical properties of this envelope type are examined in the following.

2. The S-layer-membrane system

2.1. S-layer-membrane system: Description

The osmotic behaviour of a hypothetical cell without any cell wall component (and disregarding other mechanisms of osmotic adaptat-

ion) is compared to that of a model cell, possessing an S-layer of the *Crenarchaeota* type. The basic features of the S-layer building block (Fig. 1B,C) were inspired by the S-layer unit Tetrabrachion from *Staphylothermus marinus* (Peters et al., 1996) and by the architecture of related structures (Baumeister et al., 1989; Baumeister and Lembcke, 1992).

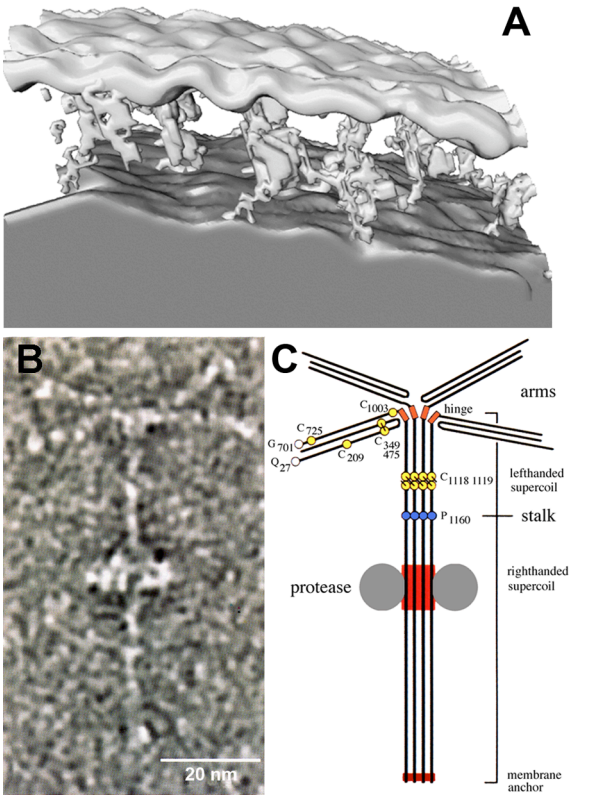

Fig. 1 S-layer of the *Crenarchaeota* type. (A) Three-dimensional representation of the S-layer from *Pyrodictium abyssi* obtained by cellular cryo-electron tomography. The structures in the quasi-periplasmic space originate from the S-layer stalks anchoring the layer in the cytoplasmic membrane and from additional, unidentified material. The image was kindly provided by Stephan Nickell, Martinsried. (B) Electron micrograph of a negatively stained S-layer unit (Tetrabrachion) forming the S-layer in *Staphylothermus marinus*. (C) Scheme of the Tetrabrachion structure. Images B and C were adapted from Peters et al. (1996).

The two model cells, i.e. essentially lipid vesicles, and characteristic stages of osmotic effects are illustrated in Fig. 2. A hypertonic vesicle interior enforces the net influx of water, which increases the vesicle volume, its surface area, and its diameter. A corresponding test system is used to determine the influx of substrates through membrane pore proteins (Zimmermann and Rosselet, 1977). Water influx continues until the increasing membrane tension prevents further extension and compensates for the developing intravesicular pressure (turgour) ΔP, or the membrane becomes leaky and disrupts (Koslov and Markin, 1984; Idiart and Levin, 2004). In principle, the same is valid for vesicles containing membrane proteins. The membrane-anchored S-layer is dilated together with the lipid membrane until the S-layer is stretched such that further expansion is impossible or the S-layer connections break. If the lateral contacts are stable, the diameter of the S-layer-cell system remains constant, but if possible influx of water will continue and expand the lipid membrane further until the membrane tension is high enough to balance the turgour. The hydrophobic S-layer anchors are fixed in place after the initial expansion. Interacting lipid molecules, surrounding the anchors, cannot move outwards since the S-layer stalk is hydrophilic beyond the membrane-spanning region. The stalk of Tetrabrachion, e.g., possesses highly polar and charged amino acid residues close to the membrane surfaces (Peters et al., 1996). Transfer of hydrophobic residues into the aqueous environment is energetically demanding and will not happen until the membrane is destroyed (Jensen and Mouritsen, 2004).

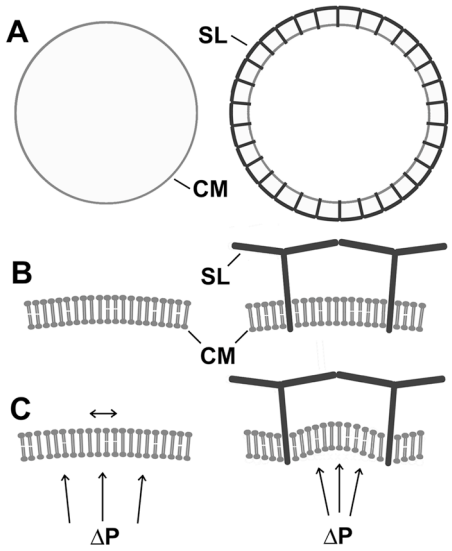

Fig. 2 Effects of internal pressure on the lipid membrane of model cells, covered by an S-layer of the Crenarchaeota type (right lane) and without any cell wall components (left lane). (A) Cell models, (B) model of a section of the cell membrane (CM) and anchoring of the S-layer (SL) at low internal pressure. (C) High internal pressure (ΔP) dilates the cell membrane of the uncovered cell, increases the cell radius and decreases the membrane curvature accordingly. The S-layer anchors hold the interacting membrane lipids in place. Intracellular pressure creates membrane bulges between the anchors and increases the membrane curvature locally.

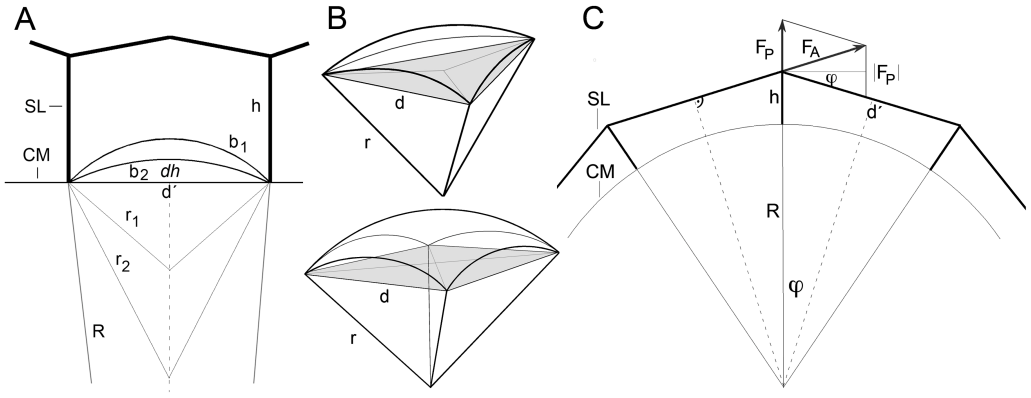

Fig. 3 Geometric consequences of bulge formation and force transmission. (A) Bulge formation of the cell membrane (CM) between S-layer (SL) anchors. R: cell radius (excluding S-layer); b_1, b_2: membrane bulges at different pressures with corresponding radii r_1, r_2; h: height of S-layer; dh: bulge height; d´: characteristic distance of S-layer anchors, where d´= {d, d√2} with tetragonal symmetry. (B) Bulge sections of S-layer unit cell size for hexagonal and tetragonal symmetry (d: lattice constant, r: bending radius). The grey membrane area is bent and expanded upon bulge formation. The minimum radii for bulges are indicated as faint lines in the grey areas. (C) Geometric consideration of forces acting on S-layer connections upon internal pressure. The force F_P is the integrated force per unit cell area originating from internal pressure ΔP. The force is completely transmitted to the S-layer and acts as pulling force F_A on the lateral S-layer connections. See Eq. 5 for the relationship between forces and S-layer geometry.

This feature not only stabilises the S-layer anchors inside the membrane matrix, but *vice versa* also immobilises the membrane relative to the protein anchors. Membrane extension should now only be possible in areas between the S-layer stalks, eventually leading to membrane bulges (Fig. 2).

2.2. S-layer-membrane system: Biophysical properties

Koslov and Markin (1984) related the size of lipid vesicles to osmotic swelling and vesicle stability. They derived an equation (Eq. 1) for the critical, i.e. maximum, intravesicular pressure ΔP^* (and the critical concentration difference of osmotically active solutes Δc^*) that a lipid membrane can withstand without forming leaks (pores).

Eq. 1 $$\Delta P^* = 3\,(K_S/r_0)\cdot(\gamma / (K_S \cdot r_0))^{2/3}$$
$$\Delta c^* = 3\,(K_S/(RT\cdot r_0))\cdot(\gamma / (K_S \cdot r_0))^{2/3}$$

The parameter K_S denotes the elasticity (compressibility or elastic area expansion) constant of ≈ 0.1–0.2 N/m for lipid membranes (Evans and Rawicz, 1990), r_0 is the vesicle radius, γ the linear tension of a pore formed by supercritical pressure ($\gamma \approx 2\cdot10^{-11} - 5\cdot10^{-11}$ N; Koslov and Markin, 1984; Sackmann, 1995). R is the gas constant, i.e. 8.31 J/(mol·K) and T the absolute temperature. It is obvious and well known that smaller vesicles are more resistant to osmotic pressure than larger ones. In fact, hypothetical cells of 100 nm in diameter or less could probably do without a cell wall. They would be stable against intracellular pressure of $1.5\cdot10^5$–$3.5\cdot10^5$ Pa (≈ 1.5–3 atm) while lipid vesicles of prokaryotic size (r = 500 nm) are destroyed above $0.03\cdot10^5$–$0.075\cdot10^5$ Pa according to Eq. 1.

The effect of bulging takes advantage of the partition of the cell membrane into apparently separated patches, i.e. the unit cell areas of the S-layer defined by the positions of the protein anchors. Membrane dilation would create rows of bulges with bending radii $r < R$ (cell radius without S-layer) that are related to the S-layer lattice constant d. The theoretical limits are $1/2\,\sqrt{2}\cdot d \le r \le R$ and $1/3\,\sqrt{3}\cdot d \le r \le R$ for $p4$ and $p6$ symmetry, respectively, as illustrated in Fig. 3. However, r presumably cannot achieve its theoretical minimum for steric reasons. In the extreme case the bulges are half-spheres and stable insertion of S-layer stalks would become a problem (Fig. 3). The hypothetical lower limit is possibly more close to $r \approx d$.

The theoretical description of bulging, i.e. formation of small vesicular deformations from (almost) planar membranes with a defined area, essentially includes two energy-dependent processes – membrane bending and expansion. Pre-bending of a membrane can be accounted for

by subtracting the curvature, originating from the cell radius *R*, from the curvature of the bulges. The basic equations Eqs. 2 and 3 define the energies for a planar piece of membrane that is either bent or stretched in plane (Sackmann, 1995). As a first approximation, I use these expressions to assess the energies for bulge formation. To obtain relationships between ΔP and the expressions in Eqs. 2 and 3 it is taken into account that the work exerted by the internal pressure increases the volume by dV (Eq. 4) and equals the bending or extension energy at equilibrium. The real pressure is a function of both contributions (but not necessarily the simple sum).

Eq. 2 $E_B = 1/2\ \kappa_C\ (2/r - c)^2 \cdot A_O$
Eq. 3 $E_S = 1/2\ K_S\ (dA)^2 / A_O$
Eq. 4 $W = \Delta P \cdot dV = \Delta P \cdot A_O \cdot f(dh)$

Here, κ_C denotes the bending stiffness of $\approx 10^{-19}$ Nm (Evans and Rawicz, 1990; Sackman, 1995), K_S the elasticity modulus of ≈ 0.2 N/m (Evans and Rawicz, 1990), *r* the bending radius, where 2/*r* is the curvature in both directions and *c* the curvature of prebending (e.g., 2/*R* for a spherical cell), A_O is the original membrane area under consideration, and dA the gain in area upon stretching. The parameter $f(dh)$ in Eq. 4 is a function of *dh*, i.e. the height of the bulge relative to the original membrane level. The calculations for the curves in Fig. 4 were made using a model membrane stabilised by a tetragonal S-layer of lattice constant *d*. For the sake of simplicity, it was assumed that the 'unit cell' has a circular shape with a diameter of $d \cdot \sqrt{2}$. Nevertheless, this approximation still leads to reasonable estimates since the curvature of the bent membrane remains the same for the real and the model unit cells, and the increase of the membrane area *dA* (Eq. 3) is normalised to the corresponding projection area and is at least partly corrected for the larger model unit cell.

Fig. 4A illustrates that the contributions of bending and expansion forces critically depend on the unit cell size (lattice constant) of the S-layer. The bending energy is dominant in the low pressure regime with small unit cells (*d* = 15 nm) while expansion forces become demanding with bulges at higher curvature (*r* < 40 nm). The situation changes with larger unit cells (*d* = 30 nm). Now, bending forces are less important and membrane dilation requires more energy below a curvature radius of ≈ 70 nm. In general, the pressure increases considerably beyond *r* ≈ 50 nm, indicating the region for the most efficient size of membrane bulges with respect to pressure resistance. Interestingly, the smallest radii possible for S-layer-armed membranes, i.e. ≈ 15–35 nm (see above and Tab. I), apparently provide a pressure stability for ΔP higher, or even much higher, than $2 \cdot 10^5$ Pa. Lipid vesicles of comparable radii are stable at corresponding pressures (Eq. 1).

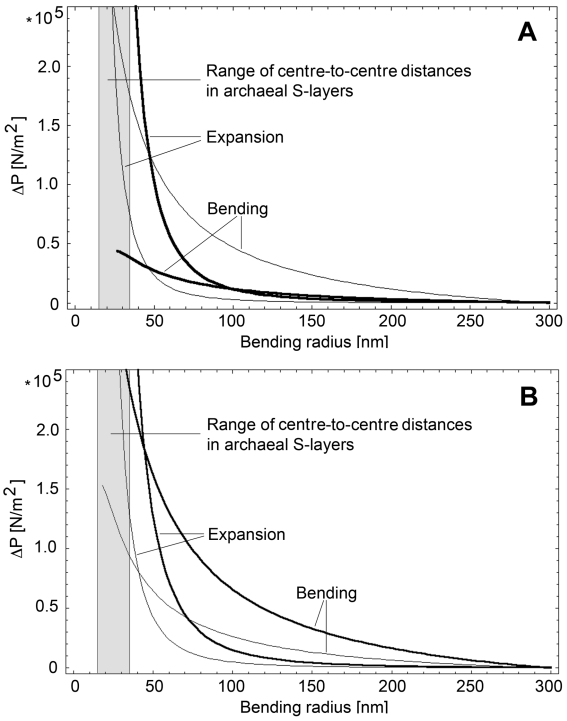

Fig. 4 Theoretical calculations of the effects of positive internal pressure ΔP on membrane patches of lipid vesicles possessing S-layers of the Crenarchaeota type. The curves are based on the Eqs. 2-4. Membrane bending and membrane expansion are treated as independent effects from an energetic viewpoint. The amount of area expansion is calculated as a function of membrane bending, assuming that the internal pressure creates membrane bulges of bending radius *r* between the anchors of a tetragonal S-layer unit cell. The lattice constants of the S-layers are (A) 15 nm (fine curves), 30 nm (bold curves), and (B) 20 nm. The calculations were made for lipid membranes with a moderate bending stiffness of $\kappa_C = 10^{-19}$ Nm and an elasticity modulus of K_S = 0.2 N/m in (A) and in (B) for the curves displayed with fine lines, and for stiff membranes with $\kappa_C = 2.5 \cdot 10^{-19}$ Nm and K_S = 0.6 N/m in (B) represented by the bold curves. The calculations were performed using *Mathematica* 4.1 (Wolfram Research Inc.).

Evans and Rawicz (1990) derived a model, combining the bending and stretching effects for giant lipid vesicles and large bulges extruded by a micropipette. They also observed that the effects of membrane expansion dominated with increasing pressures (Fig. 4B) and determined the elasticity moduli for various types and compositions of lipids. The quantitative effects of membrane stability obviously depend on a number of parameters (temperature, elasticity and bending moduli etc.) that may vary among different archaeal species. This and the fact that the models available were derived for vesicles on a length scale of micrometres rather than of nanometres, make quantitative interpretations difficult. Nevertheless, these considerations offer insight into the rationale of S-layer-membrane assemblies (Section 2.4.).

2.3. S-layer stability: Quantitative estimates

The osmoprotectant model implies that the lateral connections of S-layers are strong enough to compensate for the forces acting on them in the course of a positive ΔP inside the cell (Fig. 3C). For the sake of simplicity, I assume that the force pressing on an area of unit cell size is completely transmitted to the S-layer stalk and to the S-layer connections, which is not exactly true if the membrane deforms and dissipates energy.

The sketch in Fig. 3C relates the forces to the geometry of the S-layer-membrane assembly and illustrates how to derive Eq. 5. Here, F_P denotes the force originating from the internal pressure ΔP, and ΣF_A the sum of pulling forces that exert an effect on lateral S-layer connections (arms). A_{UC} is the unit cell area of the S-layer, d' its lattice constant or a related distance, R the cell radius without S-layer, and R_C including the S-layer of height h, the latter defining the apparent periplasmic space.

Eq. 5 $F_P = \Delta P \cdot A_{UC}$

$\Sigma F_A = \Delta P \cdot A_{UC} \cdot (R + h)/d' = \Delta P \cdot A_{UC} \cdot R_C/d'$

where $\sin(\varphi/2) = F_P/(2F_A)$,

$\sin(\varphi/2) = d'/(2(R+h))$, and $R_C = R+h$

The distance d' between the stalks of neighboring unit cells measured in the direction of the connecting arms does not necessarily equal the lattice constant d. For $p4$ symmetry, d' may assume the values of d and $d\sqrt{2}$ depending on the geometry of the S-layer, but it is sufficient to use d for estimations of the upper force limits. Given the values for a number of archaeal S-layers listed in Tab. I, and here omitting the sheath of *Methanospirillum hungatei*, the range of pulling forces can be assessed as $2300\ \mathrm{nm}^2 \cdot \Delta P \le \Sigma F_A \le 13600\ \mathrm{nm}^2 \cdot \Delta P$, i.e., ≈ 0.2–1.4 nN for a net pressure of 10^5 Pa (≈ 1 atm). The force F_A for a single connection is reduced by the number of connecting arms according to the symmetry of the S-layer. The resulting range is ≈ 0.04–0.25 nN using the examples given in Tab. I.

The lateral binding forces of S-layer connections are unknown. Qualitative observations demonstrated that isolated S-layer sheets may be very stable, e.g. the envelopes from *Thermoproteus tenax* (Wildhaber and Baumeister, 1987), or apparently quite labile, depending on the treatment during preparation. So, the S-layers of *Haloferax volcanii* and of other halobacteria need divalent cations for integrity and dissociate upon the addition of chelating agents (Kessel et al., 1988; Trachtenberg et al., 2000).

Atomic force measurements and molecular dynamics calculations revealed the forces of antibody-antigen binding, between biotin and avidin, and of single covalent bonds to lie in the range of 0.2–1 nN as determined for a certain energy load rate (Grubmüller et al., 1996; Janshoff et al., 2000; Müller, 2006). The apparent binding forces are a function of the pulling velocity; they increase the faster the disruption force that is applied (Rief et al., 1997; Paci et al., 2001; Rief and Grubmüller, 2001). This may be of relevance for S-layers if they have to cope with rapid fluctuations of osmotic pressure. A recent study on AFM force measurements (Lévy and Maaloum, 2005) showed that binding systems with multiple contacts are particularly stable. That the measured stability is higher than the sum of forces of the single bonds suggests that broken bonds reform during a correspondingly slow separation process (permanent pressure). Multiple contacts between protein units are usual for S-layers. Electron microscopical investigations have shown that neighboring S-layer units are generally connected by several binding sites or extended binding areas (Fig. 5).

Archaeal S-layers are thus adequately designed to withstand forces of several nN, corresponding to pressure differences in the range of 10^5 – 10^6 Pa or higher (see above). The elastic behavior and stability of membranous material can be determined by means of AFM (Vinckier and Semenza, 1998). The few studies

Table I Geometric properties of S-layers from selected archaea

Species	Cell radius[1] R_C [nm]	Symmetry of S-layer	Lattice constant d [nm]	Unit cell A_{UC} [nm^2]	Height[2] h [nm]	Ratio[3] $A_{UC} \cdot R_C/d$ [nm^2]	Reference[4]
Methanospirillum hungatei[5]	220	*p*1 or *p*2	5.7 or 2.8 (85.6°)	15.9		615 or 1250	Xu et al., 1996
Methanoplanus limicola	plane	*p*6	14.7	187	5 – 10		Cheong et al., 1991
Nanoarachaeum equitans	250	*p*6	15	195	20	3 300	Huber et al., 2002
Halobacterium salinaurm	400	*p*6	15	195	10	5 200	Trachtenberg et al., 2000
Square bacterium	plane	*p*6	≈ 16	≈ 222	≈ 20		Kessel and Cohen, 1982
Haloferax volcanii	disc-shaped	*p*6	16.8	244	10		Kessel et al., 1988
Archaeoglobus fulgidus	900	*p*6	17.5	265	≈ 30	13 600	Kessel et al., 1990
Desulfurococcus mobilis	450	*p*4	18	324		8 100	Wildhaber et al., 1987
Sulfolobus acidocaldarius	500	*p*3	21	378	25	9 100	Stetter and Zillig, 1985
Hyperthermus butylicus	500	*p*6	25	541	20	10 800	Baumeister et al., 1990
Thermofilum pendens	100	*p*6	27	631		2 300	Stetter and Zillig, 1985
Thermoproteus tenax	150	*p*6	30	779	25	3 900	Stetter and Zillig, 1985
Pyrobaculum islandicum	200	*p*6	30	779	30	5 200	Phipps et al., 1990
Staphylothermus marinus	400	*p*4	≈ 35	≈ 1225	70	≈ 9 900[6]	Peters et al., 1995

1) spherical or cylindrical radius including S-layer, data represent characteristic or approximate values
2) "periplasmic space"
3) see Eq. 5 and text
4) major reference; data may represent compilations from several sources
5) protein sheath, not membrane-anchored
6) using $d' = d \cdot \sqrt{2}$ for calculation (see Eq. 5 and text)

available revealed values of the elasticity modulus (Young´s modulus) of living cells or isolated cell envelopes to lie within a range that appears to allow for a pressure of $85 \cdot 10^5$–$150 \cdot 10^5$ Pa for the Gram-negative bacterium *Magnetospirillum gryphiswaldense* (Arnoldi et al., 2000) and of ≥ $300 \cdot 10^5$ Pa for the protein sheath of *M. hungatei* (Xu et al., 1996). According to the calculations based on Eq. 5 and the values in Tab. I, the protein connections per unit cell of the sheath must resist lateral forces of 18–40 nN. On the other hand, studies with *Methanococcus jannaschii,* an Euryarchaeon possessing an S-layer of the *Crenarchaeota* type (Beveridge and Schultze-Lam, 1996), showed that cells grown at $260 \cdot 10^5$ Pa gas pressure were ruptured if decompression was too fast, but cells taken from cultures at $7.8 \cdot 10^5$ Pa remained intact (Park and Clark, 2002), which is in agreement with the quantitative assessment outlined above. The turgour of various Gram-negative bacteria is in the range of ≈ $1 \cdot 10^5$–$6 \cdot 10^5$ Pa as determined by means of the gas vesicle approach (Koch and Pinette, 1987; Beveridge, 1988; Overmann et al., 1991). The theoretical considerations as well as the experimental results published to date suggest that archaeal S-layers are indeed stable enough to withstand the forces induced by (fluctuations of) osmotic pressure.

2.4. Functional impact of the S-layer unit cell size

Subdividing the cytoplasmic membrane into small and apparently independent patches stabilises the lipid envelope against intracellular pressure by about two orders of magnitude compared to pure lipid vesicles of cellular size. Whether the membrane becomes significantly bulged at higher pressure depends on the membrane tension that is characterised by the moduli for bending and area expansion. These moduli represent material constants and vary with the lipid composition (Evans and Rawicz, 1990; Needham and Nunn, 1990; Rutkowski et al., 1991). Membranes made of etherlipids are stiffer than those containing phosphatidylcholines (Baba et al., 1999). In addition, the effects of other membrane proteins and charged head groups in conjunction with the ionic milieu as well as the temperature (thermophiles!) have to be taken into account. Since the elasticity of native archaeal membranes under natural conditions remains to be determined, I can only make guesses. Membranes with moderate moduli as used in the model calculations should allow for bulge radii of ≈ 50–80 nm (Fig. 4), resulting in vertical membrane extensions of ≈ 0.4–2.5 nm depending on the S-layer symmetry and lattice constants. However, the putative bulge height of stiff membranes might not exceed a few Ångströms even at higher pressures (Fig. 4B).

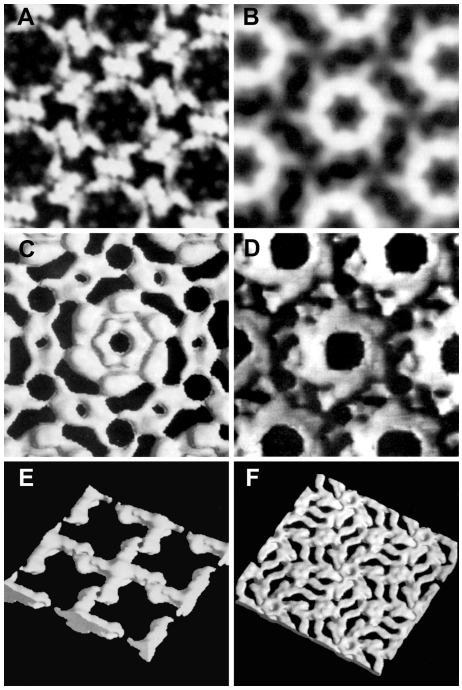

Fig. 5 View of the outer surface of S-layer structures from various archaea as obtained from electron microscopical 3-D reconstructions. The morphological units are connected by extended and multiple contact sites. S-layer structures are from (A) *Sulfolobus acidocaldarius* (Lembcke et al., 1991), (B) *Haloferax volcanii* (formally *Halobacterium volcanii*) (Kessel et al., 1988), (C) *Hyperthermus butylicus* (Baumeister et al., 1990), (D) *Methanoplanus limicola* (Cheong et al., 1991), (E) *Desulfurococcus mobilis* (Wildhaber et al., 1987), and (F) *Pyrobaculum islandicum* (Phipps et al., 1990) (data are presented with permission). For lattice constants see Tab. I.

Systematic membrane deformations of ≈ 1 nm were probably large enough to be detected by means of cryo-electron tomography (Baumeister, 2005; Lucic et al., 2005; Plitzko and Engelhardt, 2005). Fig. 1A shows similar membrane undulations of unknown source in the tomogram of *Pyrodictium abyssi.* Cryo-electron tomography thus offers a way to determine such effects experimentally on a length scale of nanometres as a possible complement to measurements on the micrometer scale (Evans and Rawicz, 1990). S-layer-covered vesicles extruded from archaea, e.g. *Pyrodictium abyssi* (Frangakis and Hegerl, 2002), or artificially reconstituted ones could serve as experimental models.

The membrane response to internal pressure clearly depends on the S-layer unit cell size (Fig 4). Cells that take advantage of a pressure-resistant membrane should, therefore, prefer S-layers with small centre-to-centre distances and *p*6 instead of *p*4 symmetry. This is the case for halophilic archaea, e.g., *Halobacterium*, *Haloferax*, and Walsby´s Square Bacterium (Tab. I). Halobacteria exhibit a high intracellular concentration of K^+ and of other compatible solutes (Martin et al., 1999; Müller et al., 2005) that would give rise to water influx if the environment became suddenly diluted (rain!). A simple experiment demonstrates the osmo-protectant function of intact S-layers with *H. salinarum* (Fig. 6). Cells that are depleted in Mg^{2+} lose the integrity of their S-layer lattice (Kushner, 1964; Mescher and Strominger, 1976; König et al., 2007) become osmosensitive upon dilution of the salt medium and lyse (Fig. 6D), while cells possessing an uninjured S-layer are resistant and preserve a rod-like shape (Fig. 6C). However, the globular swelling at the cell pole discloses the 'Achilles heel' of the S-layer. Unavoidable lattice imperfections at the pole caps (Pum et al., 1991; Wildhaber and Baumeister, 1987) affect the interaction of S-layer units, weaken the lateral stability and, obviously, the resistance of the S-layer-membrane system against intracellular pressure. The energetic aspects of lattice imperfections in archaeal and bacterial S-layers have still to be elucidated.

Another consequence of small S-layer unit cells is the relatively strong bending resistance of the respective membrane patches (Fig. 4). If the cells are not exposed to osmotic imbalance, and the lipids or other cellular factors (Sackmann, 1995; Møller-Jensen and Löwe, 2005; Zimmerberg and Kozlov, 2006) do not force strong pre-bending of the membrane, the S-layer-membrane assembly would assume a shape approaching the tension minimum, i.e., a flat, sheet-like arrangement in the ideal case. A model system shown in (Engelhardt, 2007) illustrates the expected effect. The reconstituted S-layer of *Delftia acidovorans* (*p*4 symmetry, lattice constant 10.5 nm), interacts with the membrane via bound lipid molecules (Engelhardt et al., 1991) and flattens the symmetrical lipid layer of the vesicles. Interestingly, disk-like species such as *Haloferax volcanii* and *Methanoplanus limicola*, or archaea forming flat cellular boxes ('Square Bacterium') do possess S-layers with *p*6 symmetry and particularly short lattice constants (14.7–16.8 nm; Tab. I). Although other, possibly unknown mechanisms might contribute to the architecture of archaeal cells, it is conceivable that the biophysical properties of the S-layer-membrane assembly are sufficient to flatten cells (Engelhardt, 2007).

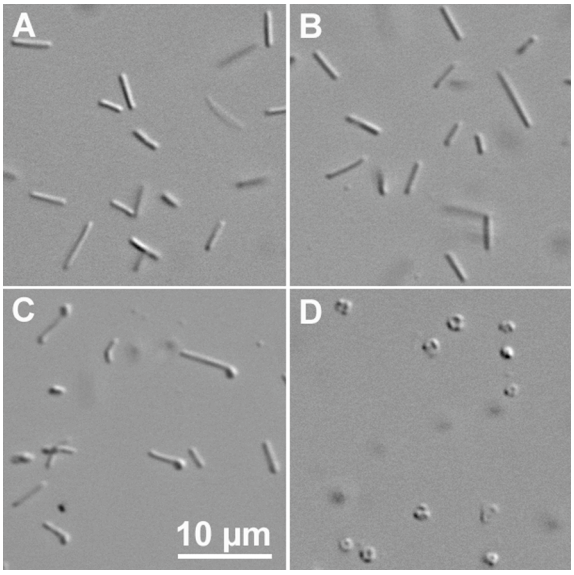

Fig. 6 *Halobacterium salinarum* (strain R1) exposed to solutions with different salt concentrations. Cells in growth medium were rapidly mixed 1:1 with salt solutions yielding final concentrations of (A) 4.27 M NaCl, 80 mM $MgSO_4$ (control), (B) 4.27 M NaCl, 40 mM $MgSO_4$, (C) 2.14 M NaCl, 80 mM $MgSO_4$, (D) 2.14 M NaCl, 40 mM $MgSO_4$, 80 mM EDTA (for Mg^{2+} chelation). All samples contained 27 mM KCl, 5 mM tri-sodium citrate, and 5 g/L peptone in addition. Note that Mg^{2+}-depleted cells (sample D) lose the lateral integrity of their S-layer lattice, and a sudden drop of the NaCl concentration results in a jump of the cell turgour (samples C and D).

An interesting aspect of this analysis is that the lattice constants and symmetries of S-layers become functionally significant in S-layer-membrane assemblies. This is not only implied by the biophysical system described in Section 2.2, but can also be derived from Eq. 5. The binding force ΣF_A between neighbouring S-layer units that compensates for the turgor ΔP is proportional to R_C and to A_{UC}/d'. A given stability of lateral contacts in S-layers is thus particularly effective (i) if the cell radius R_C is small (an aspect that has not been recognised yet), and (ii) if A_{UC}/d' is minimal. Since A_{UC}/d' is proportional to $d \cdot \sin(\alpha)$, where α is the symmetry angle of the S-layer unit cell (e.g. 60° for $p6$), it becomes immediately clear that a small lattice constant d and a high symmetry is optimal. Short lattice constants and a hexagonal arrangement of protein units have the advantage of providing a high density of contact sites per area and, concomitantly, a higher lateral stability. Furthermore, S-layers with hexagonal symmetry benefit from more contact sites per unit area particularly in regions with lattice faults, i.e. the most fragile lattice arrangement, because omitting one regular contact means still having five left, even if they are not regular, but only three in the case of $p4$ lattices. It is probably not mere chance that *Archaea* predominantly exhibit S-layers with $p6$ symmetry (Sára and Sleytr, 2000).

2.5. Variants of S-layer-membrane interactions

Archaea developed different cell wall architectures during evolution and not all of the species rely on S-layers alone (König, 1994; Kandler and König, 1998; König et al., 2007). It is intuitively imaginable and was verified experimentally in one case that the pseudomurein layers of *Methanothermus, Methanopyrus* and of the *Methanobacteriales*, the sheath of *Methanospirillaceae* (Xu et al., 1996), and the polysaccharide layers of *Natronococcus* and *Halococcaceae* are stable cell wall structures that resist osmotic stress. Interestingly, cells of *Methanospirillum hungatei* are covered by an S-layer inside the stable sheath. The S-layer is not thought to add to the osmotic stability (Firtel et al., 1993). A few species apparently lack S-layers and are defined as cell wall-less, such as *Thermoplasma acidophilum* and *Ferroplasma acidiphilum* (Darland et al., 1979; Golyshina et al., 2000). However, *T. acidophilum* possesses high amounts of a membrane glycoprotein (Yang and Haug, 1979) that could form a membrane or surface protein layer; its molecular organisation remains to be established. An interesting alternative or variant for membrane support is the contribution of membrane proteins forming networks within the lipid bilayer (Engelman, 2005). There are examples for extended patches of membrane proteins, e.g. the bacteriorhodopsin in halobacteria (Henderson, 1975) and pore protein complexes in the outer membrane of *Ignicoccus hospitalis*, the only archaeon known to possess an outer membrane but no S-layer (Huber et al., 2000; Rachel et al., 2002; Burghardt et al., 2007). Their effects on membrane stability, however, have not been characterised yet.

The association of surface proteins with lipid molecules or anchoring by means of covalently bound fatty acids residues is an apparently natural situation for some S-layers (Engelhardt and Peters, 1998). The glycosylated surface proteins of *H. salinarum* and *H. volcanii* are modified by lipids, which presumably contribute to membrane anchoring in addition (Kikuchi et

al., 1999; Konrad and Eichler, 2002). The mere non-covalent interaction of archaeal S-layers with the head groups of membrane lipids is still hypothetical but could contribute to membrane stability in *Euryarchaeota* (Schuster et al., 1999; Schuster and Sleytr, 2002; Engelhardt, 2007). The mutual effects between the S-layer and other components of the cell envelope remain to be elucidated.

3. Conclusion

Cell envelope stability is not a feature *per se* of a single cell envelope component. Rather, it is a synergistic function of interacting cell envelope layers. Its mechanism as well as the significance for mechanical and osmotic cell stabilisation must be elucidated in conjunction with the interacting molecular partners and its macromolecular assemblies (Engelhardt, 2007). The archaeal S-layer-membrane system analysed here revealed principles of the S-layer architecture that may also play a role in S-layer-outer membrane and S-layer-peptidoglycan associations in bacteria. We will learn more about general aspects of S-layer functions if we look at the cell envelope as an integrated structural assembly, and not only as an ordered succession of independent layers covering the cell.

Acknowledgements

I thank Reinhard Guckenberger and Reiner Hegerl (Department of Structural Molecular Biology, MPI of Biochemistry), Thomas Rädler (Physics Department, University of Munich), Erwin Galinski (Institute of Microbiology and Biotechnology, University of Bonn) for valuable discussions, and Andrew Leis (MPI of Biochemistry) for critically reading the manuscript.

References

Arnoldi, M., Fritz, M., Bäuerlein, E., Radmacher, M., Sackmann, E., Boulbitch, A., 2000. Bacterial turgour pressure can be measured by atomic force microscopy. Phys. Rev. E 62, 1034-1044.

Baba, T., Toshima, Y., Minamikawa, H., Hato, M., Suzuki, K., Kamo, N., 1999. Formation and characterization of planar lipid bilayer membranes from synthetic phytanyl-chained glycolipids. Biochim. Biophys. Acta 1421, 91-102.

Baumeister, W., 2005. From proteomic inventory to architecture. FEBS Lett. 579, 933-937.

Baumeister, W., Wildhaber, I., Phipps, B.M., 1989. Principles of organization in eubacterial and archaebacterial surface proteins. Can. J. Microbiol. 35, 215-227.

Baumeister, W., Santarius, U., Volker, S., Dürr, R., Lembcke, G., Engelhardt, H., 1990. The surface protein of *Hyperthermus butylicus*: Three dimensional structure and comparison with other archaebacterial surface proteins. System. Appl. Microbiol. 13, 105-111.

Baumeister, W., Lembcke, G., 1992. Structural features of archaebacterial cell envelopes. J. Bioenerget. Biomembr. 24, 567-575.

Beveridge, .TJ., 1988. The bacterial surface: general considerations twoards design and function. Can. J. Microbiol. 34, 363-372.

Beveridge, T.J., Schultze-Lam, S., 1996. The response of selected members of the archaea to the Gram stain. Microbiol. 142, 2887-2895.

Blount, P., Sukharev, S.I., Moe, P.C., Nagle, S.K., Kung, C., 1996. Towards an understanding of the structural and functional properties of MscL, a mechanosensitive channel in bacteria. Biol. Cell. 87, 1-8.

Burghardt, T., Näther, D.J., Junglas, B., Huber, H., Rachel, R., 2007. The dominating outer membrane protein of the hyperthermophilic Archaeum *Ignicoccus hospitalis*: a novel pore-forming complex. Mol. Microbiol. 63, 166-176.

Cheong, G.-W., Cejka, Z., Peters, J., Stetter, K.O., Baumeister, W., 1991. The surface protein layer of *Methanoplanus limicola*: Three-dimensional structure and chemical characterization. System. Appl. Microbiol. 14, 209-217.

Darland, G., Brock, T.D., Samsonoff, W., Conit, S.F., 1970. A thermophilic, acidophilic mycoplamsa isolated from a coal refuse pile. Science 170, 1416-1418.

Engelhardt, H., 2007. Are S-layers exoskeletons? The basic function of protein surface layers revisited. J. Struct. Biol. (online) DOI: 10.1016/j.jsb.2007.08003

Engelhardt, H., Peters, J., 1998. Structural research on surface layers – A focus on stability, surfacel layer homology domains, and surface layer-cell wall interactions. J. Struct. Biol. 124, 276-302.

Engelhardt, H., Gerbl-Rieger, S., Santarius, U., Baumeister, W., 1991. The three-dimensional structure of the regular surface protein of *Comamonas acidovorans* derived from native outer membranes and reconstituted two-dimensional crystals. Mol. Microbiol. 5, 1695-1702.

Engelman, D.M.,2005. Membranes are more mosaic than fluid. Nature 438, 578-580.

Evans, E., Rawicz, W., 1990. Entropy-driven tension and bending elasticity in condensed-fluid membranes. Phys, Rev, Lett, 64, 2094-2097.

Firtel, M., Southam, G., Harauz, G., Beveridge T.J., 1993. Characterization of the cell wall of the sheathed methanogen *Methanospirillum hungatei* GP1 as an S layer. J. Bacteriol. 175, 7550-7560.

Frangakis, A.S., Hegerl, H., 2002. Segmentation of two- and three-dimensionl data from electron microscopy using eigenvector analysis. J. Struct. Biol. 138, 105-113.

Göller, K., Ofer, A., Galinski, E.A.,1998. Construction and characterization of an NaCl-sensitive mutant of *Halomonas elongata* impaired in ectoine biosynthesis. FEMS Microbiol. Lett. 161, 293-300.

Golyshina, O.V., Pivovarova, T.A., Kravaiko, G.I., Kondrat´eva, T.F., Moore, E.R.B., Abraham, W.-R., Lünsdorf, H., Timmis, K.N., Yakimov, M.M., Golyshin, P.N., 2000. *Ferroplasma acidiphilum* gen. nov., sp. nov., an acidophilic, autotrophic, ferrous-iron-oxidizing, cell-wall-lacking, mesophilic member of the *Ferroplasmaceae* fam. nov., comprising a distinct lineage of the *Archaea*. Int. J. Sys. Evol. Microbiol. 50, 997-1006.

Grubmüller, H., Heymann, B., Tavan, P., 1996. Ligand binding: Molecular mechanics calculation of the streptavidin-biotin rupture force. Science 271, 997-999.

Henderson, R., 1975. The structure of the purple membrane from *Halobacterium halobium*: Analysis of the X-ray diffraction pattern. J. Mol. Biol. 93, 123-128.

Huber, H., Burggraf, S., Maye,r T., Wyschkony, I., Rachel, R., Stetter, K.O., 2000. *Ignicoccus* gen.nov., a novel genus of hyperthermophilic, chemolithotrophic Archaea, represented by two new species, *Ignicoccus islandicus* sp.nov. and *Ignicoccus pacificus* sp.nov. Int. J. Syst. Evol. Microbiol. 50, 2093-2100.

Huber, H., Hohn, M.J., Rachel, R., Fuchs, T., Wimmer, V.C., Stetter, K.O., 2002. A new phylum of *Archaea:* Represented by a nanosized hyperthermophilic symbiont. Nature 417, 63-67.

Idiart, M.A., Levin, Y., 2004. Rupture of a liposomal vesicle. Phys Rev E 69, 061922-1-8.

Janshoff, A., Neitzert, M., Oberdörfer, Y., Fuchs, H., 2000. Force spectroscopy of molecular systems – Single molecule spectroscopy of polymers and biomolecules. Angew. Chem. Int. Ed. 39, 3212-323.

Jensen, M.O., Mouritsen, O.G., 2004. Lipids do influence protein function – the hydrophobic matching hypothesis revisited. Biochim. Biophys. Acta 1666, 205-226.

Kandler, O., König, H., 1998. Cell wall polymers in *Archaea* (Archaebacteria). Cell. Mol. Life Sci. 54, 305-308.

Kessel, M., Cohen, Y. 1982. Ultrastructure of square bacteria from a brine pool in southern Sinai. J. Bacteriol. 150, 851-860.

Kessel, M., Wildhaber, I., Cohen, S., Baumeister, W., 1988. Three-dimensional structure of the regular surface glycoprotein layer of *Halobacterium volcanii* from the Dead Sea. EMBO J. 7, 1549-1554.

Kessel M., Volker, S., Santarius, U., Huber, R., Baumeister, W., 1990. Three-dimensional reconstruction of the surface protein of the extremely thermophilic archaebacterium *Archaeoglobus fulgidus*. System. Appl. Microbiol. 13, 207-213.

Kikuchi, A., Sgami, H., Ogura, K., 1999. Evidence for covalent attachment of diphytanylglycerly phosphate to the cell-surface glycoprotein of *Halobacterium halobium*. J. Biol. Chem. 274, 18011-18016.

Koch, A.L., Pinette, M.F.S., 1987. Nephelometric determination of turgour pressure in growing Gram-negative bacteria. J. Bacteriol. 169, 3654-3663.

König, H., 1994. Analysis of archaeal cell envelopes; in: Goodfellow, M., O´Donnell, A.G. (Eds.), Chemical Methods in Prokaryotic Systematics. Chichester, John Wiley & Sons, pp. 85-119.

König, H., Rachel, R., Claus, H., 2007. Proteinaceous surface layers of *Archaea:* ultrastructure and biochemistry; in: Cavicchioli R (ed): *Archaea* - Molecular and Cellular Biology. American Soc. Microbiol. Press, Washington, D.C., pp. 315-340.

Konrad, Z., Eichler, J., 2002. Lipid modification of proteins in *Archaea*: attachment of a mevalonic acid-based lipid moiety to the surface-layer glycoprotein of *Haloferax volcanii* follows protein translocation. Biochem. J. 366, 959-964.

Koslov, M.M., Markin, V.S., 1984. A theory of omotic lysis of lipid vesicles. J. Theor. Biol. 109, 17-39.

Kushner, D.J., 1964. Lysis and dissolution of cells and envelopes of an extremely halophilic bacterium. J. Bacteriol. 87, 1147-1156.

Lembcke, G., Dürr, R. Hegerl, R., Baumeister, W., 1991. Image analysis and processing of an imperfect two-dimensional crystal: the surface layer of the archaebacterium *Sulfolobus acidocaldarius* re-investigated. J. Microscopy 161, 263-278.

Lévy, R., Maaloum, M., 2005. Specific molecular interactions by force spectroscopy: From singel bonds to collective properties. Biophys. Chem. 117, 233-237.

Lucic, V., Förster, F., Baumeister, W., 2005. Structural studies by electron tomography: from cells to molecules. Annu. Rev. Biochem. 74, 833-865.

Martin, D.D., Ciulla, R.A., Roberts, M.F., 1999. Osmoadaptation in archaea. Appl. Environment. Micrbiol. 65, 1815-1825.

Mescher, M.F., Strominger, J.L., 1976. Structural (shape-maintaining) role of the cell surface glycoprotein of *Halobacterium salinarium*. Proc. Natl. Acad. Sci. USA 73, 2687-2691.

Møller-Jensen, J., Löwe, J., 2005. Increasing complexity of the bacterial cytoskeleton. Curr. Opin. Cell Biol. 17, 75-81.

Müller, D.J., 2006. Rasterkraftmikroskopie; in: Lottspeich, F., Engels, J.W. (Eds),Bioanalytik. Heidelberg, Spektrum Acad. Verlag, pp. 499-506.

Müller, V., Spanheimer, R., Santos, H., 2005. Stress response by solute accumulation in archaea. Curr. Opin. Microbiol. 8, 729-736.
Needham, D., Nunn, R.S., 1990. Elastic deformation and failure of lipid bilayer membranes containing cholesterol. Biophys. J. 58, 997-1009.

Overmann, J., Lehmann, S., Pfennig, N., 1991. Gas vesicle formation and buoyancy regulation in *Pelodictyon phaeoclathratiforme* (green sulfur bacteria). Arch. Microbiol. 157, 29-37.
Paci, E., Caflisch, A., Plückthun, A., Karplus, M., 2001. Forces and energetics of hapten-antibody dissociation: A biased molecular dynamics simulation study. J. Mol. Biol. 314, 589-605.

Park, C.B., Clark, D.S., 2002. Rupture of the cell envelope by decompression of the deep-sea methanogen *Methanococcus jannaschii*. Appl. Environm. Microbiol. 68, 1458-1463.

Peters, J., Nitsch, M., Kühlmorgen, B., Golbik, R., Lupas, A., Kellermann, J., Engelhardt, H., Pfander, J.-P., Müller, S., Goldie, K., Engel, A., Stetter, K.-O., Baumeister, W., 1995. Tetrabrachion: A filamentous archaebacterial surface protein assembly of unusual structure and extreme stability. J. Mol. Biol. 245, 385-401.

Peters, J., Baumeister, W., Lupas, A., 1996. Hyperthermostable surface layer protein Tetrabrachion from the archaebacterium *Staphylothermus marinus:* Evidence for the presence of a right-handed coiled coil derived from the primary structure. J. Mol. Biol. 257, 1031-1041.

Phipps, B.M., Engelhardt, H., Huber, R., Baumeister, W., 1990. Three-dimensional structure of the crystalline protein envelope layer of the hyperthermophilic archaebacterium *Pyrobaculum islandicum*. J. Struct. Biol. 103, 152-163.

Plitzko, J.M., Engelhardt, H., 2005. Large complexes and molecular machines by electron microscopy; in: Jorde, L.B, Little, P., Dunn, M., Subramaniam, S. (Eds), Encyclopedia of Genetics, Genomics, Proteomics and Bioinformatics. Chichester UK, John Wiley & Sons, Vol 6, pp. 2572-2578.

Pum, D., Messner, P., Sleytr, U.B., 1991. Role of the S layer in morphogenesis and cell division of the archaebacterium *Methanocorpusculum sinense*. J. Bacteriol. 173, 6865-6873.

Rachel, R., Wyschkony, I., Riehl, S., Huber, H., 2002. The ultrastructure of *Ignicoccus:* Evidence for a novel outer membrane and for intracellular vesicle budding in an archaeon. Archaea 1, 9-18.

Rief, M., Gautel, M., Oesterhelt, F., Fernandez, J.M., Gaub, H.E., 1997. Reversible unfolding of individual titin immunoglobulin domains by AFM. Science 276, 1109-1112.

Rief, M., Grubmüller, H., 2001. Kraftspektroskopie von einzelnen Biomolekülen. Phys. Blätter 57, 55-61.

Rutkowski, C.A., Williams, L.M., Haines, T.H., Cummins, H.Z., 1991. The elasticity of synthetic phospholipid vesicles obtained by photon correlation spectroscopy. Biochem. 30, 5688-5696.

Sackmann, E., 1995. Physical basis of self-organization and function of membranes: Physics of vesicles; in: Lipowski, R., Sackmann, E. (Eds.), Structure and Dynamics of Membranes. From Cells to Vesicles. Amsterdam, Elsevier, Vol 1, pp. 213-304.

Sára, M., Sleytr, U.B., 2000. S-layer proteins. J. Bacteriol. 182, 859-868.

Schuster, B., Sleytr, U.B., Diederich, A., Bähr, G., Winterhalter, M., 1999. Probing the stability of S-layer-supported planar lipid membranes. Eur. Biophys. J. 28, 583-590.

Schuster, B., Sleytr, U.B., 2002. The effect of hydrostatic pressure on S-layer-supported lipid membranes. Biochim. Biophys. Acta 1563, 29-34.

Stetter, K.-O., Zillig, W., 1985. Thermoplasma and the thermophilic sulfur-dependent archaebacteria; in: Woese, C.R., Wolfe, R.S. (Eds.), The Bacteria. A Treatise on Structure and Function. Archaebacteria. Orlando, Acad Press, Vol VIII, pp. 85-170.

Trachtenberg, S., Pinnick, B., Kessel, M., 2000. The cell surface glycoprotein layer of the extreme halophile Halobacterium salinarum and its relation to haloferax volcanii: Cryo-electron tomography of freeze-substituted cells and projection studies of negatively stained envelopes. J. Struct. Biol. 130, 10-26.

Vinckier, A., Semenza, G., 1998. Measuring elasticity of biological materials by atomic force microscopy. FEBS Lett. 430, 12-16.

Wildhaber, I., Baumeister, W., 1987. The cell envelope of *Thermoproteus tenax:* three-dimensional structure of the surface layer and its role in shape maintenance. EMBO J. 6, 1475-1480.

Wildhaber, I., Santarius, U., Baumeister, W., 1987. Three-dimensional structure of the surface protein of *Desulfurococcus mobilis*. J. Bacteriol. 169, 5563-5568.

Xu, W., Mulhern, P.J., Blackford, B.L., Jericho, M.H., Firtel, M., Beveridge, T.J., 1996. Modeling and measuring the elastic properties of an archaeal surface, the sheath of *Methanospirillum hungatei,* and the implication for methane production. J. Bacteriol. 178, 3016-3112.

Yang, L.L., Haug, A., 1979. Purification and partial characterization of a procaryotic glycoprotein from the plasma membrane of *Thermoplasma acidophilum*. Biochim. Biophys. Acta 556, 265-277.

Zimmerberg, J., Kozlov, M.M., 2006. How proteins produce cellular membrane curvature. Nature Rev. Mol. Cell Biol. 7, 9-19.

Zimmermann, W., Rosselet, A., 1977. Function of the outer membrane of *Escherichia coli* as a permeability barrier to beta-lactam antibiotics. Antimicrob. Agents & Chemotherapy 12, 368-72.